

Synthesis and crystal structure of (2*E*)-1-[3,5-bis(benzyloxy)phenyl]-3-(4-ethoxyphenyl)prop-2-en-1-one

K. R. Jeyashri,^a G. Logeshwari,^a U. Rajapandiyan,^a K. Sivakumar,^b S. Selvanayagam,^c ‡ H. Manikandan^{a*} and K. Kaviyarasu^d

Received 8 July 2024
Accepted 31 July 2024

Edited by W. T. A. Harrison, University of Aberdeen, United Kingdom

‡ Additional correspondence author, e-mail: s_selvanayagam@rediffmail.com.

Keywords: crystal structure; chalcone derivative; C—H···O interactions; Hirshfeld surface analysis.

CCDC reference: 2182630

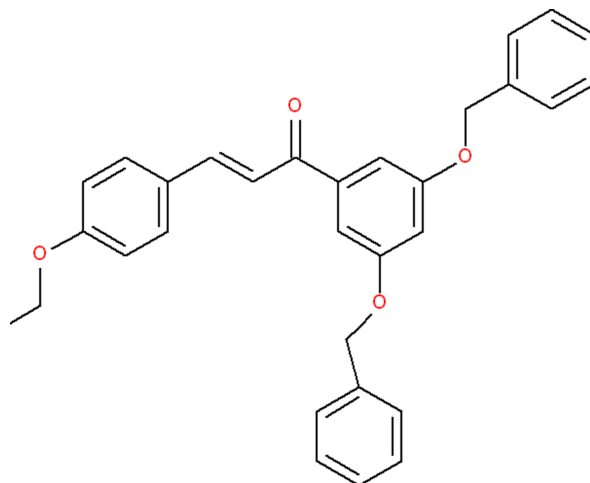
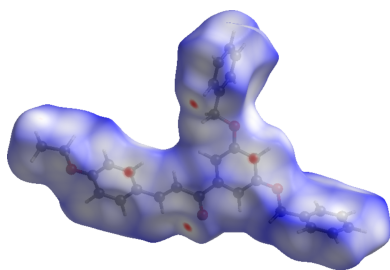
Supporting information: this article has supporting information at journals.iucr.org/e

^aDepartment of Chemistry, Annamalai University, Annamalaiagar, Chidambaram 608 002, India, ^bDepartment of Chemistry, Sri Chandrasekharendra Saraswathi Viswa Mahavidyalaya, (Deeded to be University), Kanchipuram 631 561, India, ^cPG & Research Department of Physics, Government Arts College, Melur 625 106, India, and ^dNanosciences/Nanotechnology Laboratories, University of South Africa (UNISA), Pretoria, South Africa. *Correspondence e-mail: profmani.au@gmail.com

In the title compound, C₃₁H₂₈O₄, the phenyl rings of the chalcone unit subtend a dihedral angle of 26.43 (10)°. The phenyl rings of the pendant benzyloxy groups are orientated at 75.57 (13) and 75.70 (10)° with respect to their attached ring. In the crystal, weak C—H···O and C—H···π interactions link the molecules. The intermolecular interactions were quantified and analysed using Hirshfeld surface analysis, which showed a breakdown into H···H (49.8%), H···C/C···H (33.8%) and H···O/O···H (13.6%) interactions with other types making negligible contributions.

1. Chemical context

Chalcones incorporate an α,β -unsaturated carbonyl (enone) bridge connecting two aromatic rings. The chalcone scaffold exhibits anti-cancer efficacy on various human cancer cells (Zhuang *et al.*, 2017; Liu *et al.*, 2022). DrugBank lists three chalcone-based drugs namely hesperidin methylchalcone (DrugBank: DB15943), dihydroxymethoxychalcone (DB14122) and 3-(4-hydroxyphenyl)prop-2-en-1-one (DB07500). In general, the anticancer efficacy of chalcones is enhanced by attaching different substituents at ring A of the chalcone, which is attached to the C=O group (Mai *et al.*, 2014). As part of our studies in this area, we have prepared and undertaken a single-crystal X-ray diffraction study of the title compound, C₃₁H₂₈O₄, (I), and the results are presented here.



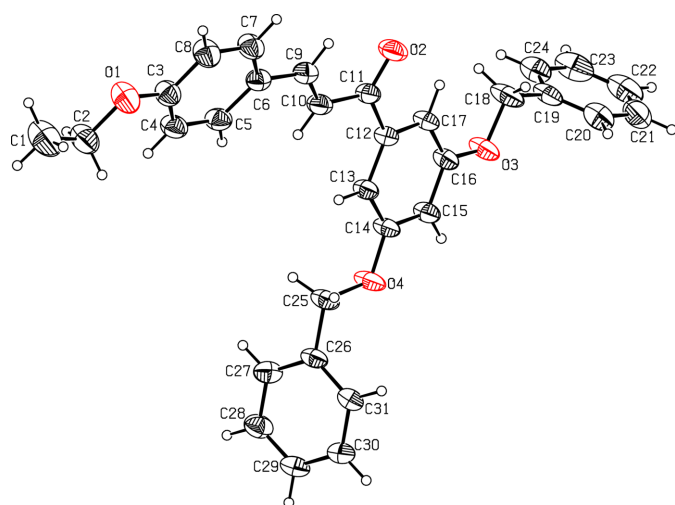


Figure 1
The molecular structure of (I) with displacement ellipsoids drawn at the 30% probability level.

2. Structural commentary

The molecular structure of (I) is illustrated in Fig. 1. The C12–C17 and C19–C24 phenyl rings of the chalcone unit subtend a dihedral angle of $26.43 (10)^\circ$: the most significant twist occurs about the C11–C12 bond, as indicated by the C10–C11–C12–C13 torsion angle of $-13.0 (3)^\circ$. The dihedral angles between the C19–C24 and C26–C31 pendant phenyl rings and their attached C12–C17 ring are $75.57 (13)$

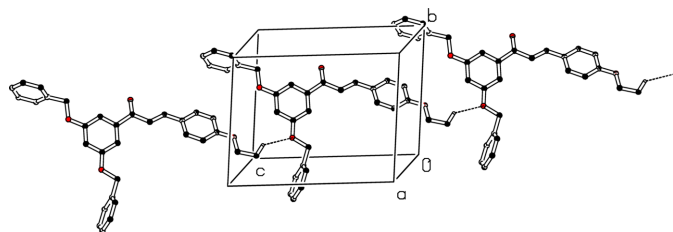


Figure 2
Detail of the packing of (I) showing C–H...O interactions as dashed lines. For clarity H atoms not involved in these hydrogen bonds have been omitted.

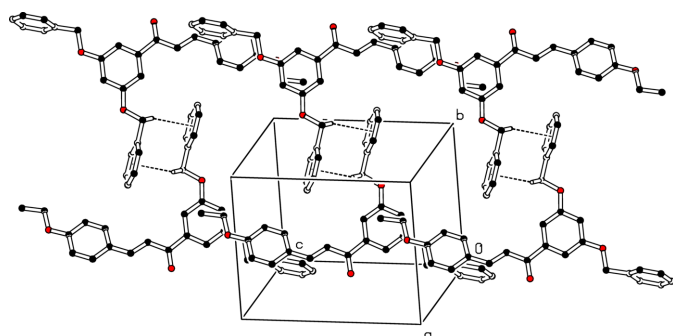


Figure 3
Detail of the packing of (I) showing C–H... π interactions as dashed lines.

Table 1
Hydrogen-bond geometry (\AA , $^\circ$).

Cg1 is the centroid of the C26–C31 ring.

| $D-H\cdots A$ | $D-H$ | $H\cdots A$ | $D\cdots A$ | $D-H\cdots A$ |
|------------------------------|-------|-------------|-------------|---------------|
| C1–H1A...O4 ⁱ | 0.96 | 2.64 | 3.227 (3) | 119 |
| C25–H25B...Cg1 ⁱⁱ | 0.97 | 2.68 | 3.398 (2) | 132 |

Symmetry codes: (i) $x - 1, y, z - 1$; (ii) $-x + 1, -y, -z + 1$.

and $75.70 (10)^\circ$, respectively. The C3–O1–C2–C1, C14–O4–C25–C26 and C16–O3–C18–C19 torsion angles of $177.2 (3)$, $176.21 (18)$ and $179.5 (2)^\circ$, respectively, indicate an *anti* conformation in each case.

3. Supramolecular features

In the crystal of (I), the molecules associate *via* weak C–H...O interactions (Table 1), forming $C(15)$ chains propagating along $[101]$ (Fig. 2). In addition, inversion-related molecules are linked by pairwise weak C–H... π interactions (Fig. 3).

4. Hirshfeld surface analysis

To further characterize the intermolecular interactions in (I), a Hirshfeld surface analysis was performed using *Crystal Explorer 21* (Spackman *et al.*, 2021) and the associated two dimensional fingerprint plots were generated. The HS mapped over d_{norm} in the range -0.09 to $+1.53$ a.u. is illustrated in Fig. 4, using colours to indicate contacts that are shorter (red areas), equal to (white areas), or longer than (blue areas) the sum of the van der Waals radii (Ashfaq *et al.*, 2021).

The overall two-dimensional fingerprint plot, Fig. 5a, and those delineated into H...H interactions (49.8%), H...C/C...H (33.8%), H...O/O...H (13.6%), C...C (1.8%) and O...C/C...O (1%) interactions are illustrated in Fig. 5b–f, respectively, together with their relative contributions to the HS. The most important interaction is H...H, which is reflected in Fig. 5b as widely scattered points of high density

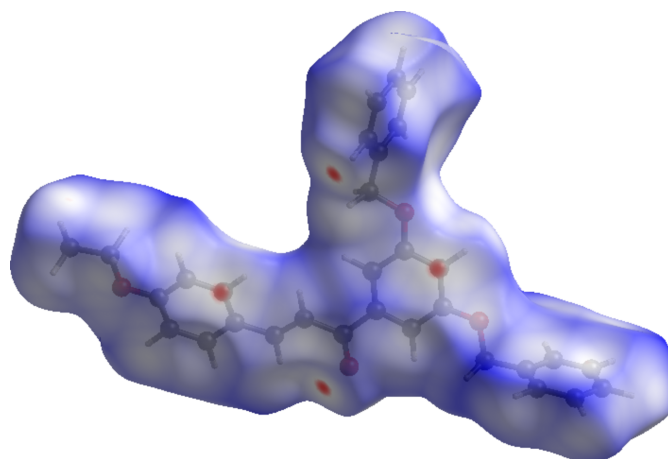


Figure 4
A view of the Hirshfeld surface mapped over d_{norm} for (I).

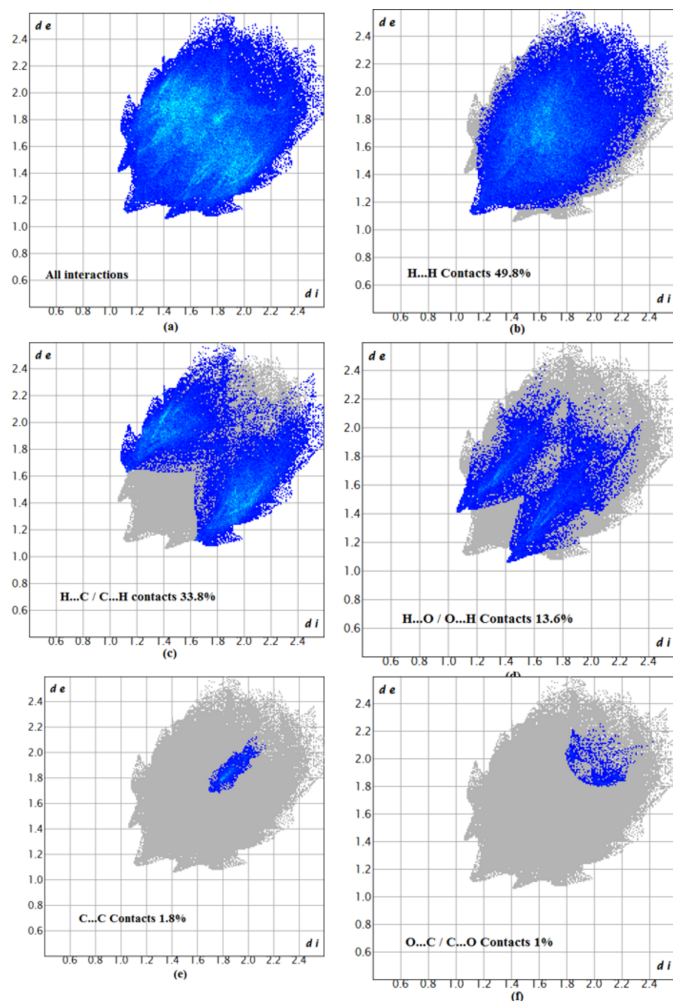


Figure 5
Two-dimensional fingerprint plots for (I), showing (a) all interactions, and delineated into (b) H...H, (c) H...C/C...H, (d) H...O/O...H, (e) C...C and (f) O...C/C...O interactions.

due to the large hydrogen content of the molecule with the tip at $d_e = d_i = 1.10$ Å. As a result of the presence of C—H...O interactions, the H...O/O...H contacts contribute 13.6% to the overall crystal packing, as reflected in Fig. 5d with the tips at $d_e + d_i = 2.50$ Å.

5. Synthesis and crystallization

Equimolar concentrations of 3,5-dibenzoyloxyacetophenone and 4-ethoxybenzaldehyde were dissolved in ethanol in separate reaction flasks and then mixed. Drop by drop, utilizing a magnetic stirring device, 2 ml of 10% sodium hydroxide in water were introduced at room temperature. The course of the process was tracked using thin-layer chromatography. After the process was complete, the resulting product was placed on crushed ice. The finished product was vacuum-filtered, dried, and then recrystallized from ethanol solution to yield colourless blocks of the title compound.

Table 2
Experimental details.

| | |
|--|--|
| Crystal data | |
| Chemical formula | C ₃₁ H ₂₈ O ₄ |
| M_r | 464.53 |
| Crystal system, space group | Triclinic, $P\bar{1}$ |
| Temperature (K) | 298 |
| a, b, c (Å) | 9.0494 (9), 10.0326 (11), 14.6932 (15) |
| α, β, γ (°) | 100.153 (3), 107.292 (3), 90.789 (4) |
| V (Å ³) | 1250.6 (2) |
| Z | 2 |
| Radiation type | Mo $K\alpha$ |
| μ (mm ⁻¹) | 0.08 |
| Crystal size (mm) | 0.31 × 0.23 × 0.19 |
| Data collection | |
| Diffractometer | Bruker D8 Quest XRD |
| Absorption correction | — |
| No. of measured, independent and observed [$I > 2\sigma(I)$] reflections | 30243, 5428, 3607 |
| R_{int} | 0.037 |
| $(\sin \theta/\lambda)_{max}$ (Å ⁻¹) | 0.638 |
| Refinement | |
| $R[F^2 > 2\sigma(F^2)]$, $wR(F^2)$, S | 0.057, 0.178, 1.05 |
| No. of reflections | 5428 |
| No. of parameters | 317 |
| H-atom treatment | H-atom parameters constrained |
| $\Delta\rho_{max}$, $\Delta\rho_{min}$ (e Å ⁻³) | 0.36, -0.18 |

Computer programs: *APEX3* and *SAINT* (Bruker, 2017), *SHELXT2018/2* (Sheldrick, 2015a), *SHELXL2019/3* (Sheldrick, 2015b), *ORTEP-3 for Windows* (Farrugia, 2012) and *PLATON* (Spek, 2020).

IR (cm⁻¹): 3032 aromatic C—H stretch, 2934 and 2875 aliphatic C—H stretch, 1651 C=O stretch, 1568 aromatic ring C=C stretch (see table in the supporting information).

6. Refinement

Crystal data, data collection and structure refinement details are summarized in Table 2. H atoms were placed in idealized positions and allowed to ride on their parent atoms: C—H = 0.93–0.97 Å, with $U_{iso}(H) = 1.5U_{eq}(C\text{-methyl})$ and $1.2U_{eq}(C)$ for other H atoms.

References

- Ashfaq, M., Tahir, M. N., Muhammad, S., Munawar, K. S., Ali, A., Bogdanov, G. & Alarfaji, S. S. (2021). *ACS Omega*, **6**, 31211–31225.
- Bruker (2017). *APEX2*, and *SAINT*. Bruker AXS Inc., Madison, Wisconsin, U. S. A.
- Farrugia, L. J. (2012). *J. Appl. Cryst.* **45**, 849–854.
- Liu, W., He, M., Li, Y., Peng, Z. & Wang, G. (2022). *J. Enzyme Inhib. Med. Chem.* **37**, 9–38.
- Mai, C. W., Yaeghoobi, M., Abd-Rahman, N., Kang, Y. B. & Pichika, M. R. (2014). *Eur. J. Med. Chem.* **77**, 378–387.
- Sheldrick, G. M. (2015a). *Acta Cryst.* **A71**, 3–8.
- Sheldrick, G. M. (2015b). *Acta Cryst.* **C71**, 3–8.
- Spackman, P. R., Turner, M. J., McKinnon, J. J., Wolff, S. K., Grimwood, D. J., Jayatilaka, D. & Spackman, M. A. (2021). *J. Appl. Cryst.* **54**, 1006–1011.
- Spek, A. L. (2020). *Acta Cryst.* **E76**, 1–11.
- Zhuang, C., Zhang, W., Sheng, C., Zhang, W., Xing, C. & Miao, Z. (2017). *Chem. Rev.* **117**, 7762–7810.

supporting information